PCCP

Accepted Manuscript

ROYAL SOCIETY OF CHEMISTRY

www.rsc.org/pccp

Short title: Ultrafast nonlinear IR spectroscopy of α-elastin coacervation

Coacervation of α-elastin studied by ultrafast nonlinear infrared spectroscopy

Elena Ragnoni,[†•] Francesca Palombo,[‡,*] Ellen Green,[‡] C. Peter Winlove,[‡] Mariangela Di Donato,[†#§] and Andrea Lapini[†§]

[†] LENS, European Laboratory for Nonlinear Spectroscopies, Via Nello Carrara 1, I-50019 Sesto Fiorentino, Florence, Italy
• Department of Physics, University of Siegen, Walter-Flex Str. 3, 57068 Siegen, Germany
[‡] School of Physics and Astronomy, University of Exeter, Exeter EX4 4QJ, UK
[#] Department of Chemistry, University of Florence, via della Lastruccia 3-13, I-50019 Sesto Fiorentino, Florence, Italy
[§] INO, National Institute of Optics, Largo Enrico Fermi 6, I-50125 Florence, Italy

Abstract

Elastin is the main protein to confer elasticity to biological tissues, through the formation of a hierarchical network of fibres. α-Elastin, a soluble form of the protein, is widely used in studies of the biosynthesis of human elastic tissue and exhibits coacervation in solution. This process involves the association of α-elastin molecules through a liquid–liquid phase transition, which is reversible unless the temperature is driven sufficiently high to induce the formation of insoluble aggregates. The thermodynamics of this process have attracted interest over many years and in the present work we used ultrafast nonlinear infrared spectroscopy of the amide I protein backbone vibration to resolve the secondary structural changes occurring during coacervation and probe the protein dynamics on a picosecond time scale. Four classes of carbonyl oscillators with distinct absorption peaks were revealed and, through narrowband excitation, vibrational and anisotropy decays could be distinguished. Analysis of the vibrational lifetimes and anisotropy decay times of these bands characterized the conformational changes and revealed the structural bases of the coacervation process.

1. Introduction

The extracellular matrix (ECM) is a complex network of fibrous proteins and other macromolecular components and provides a natural scaffold to cells in biological tissues. Elastin is one of the most ubiquitous proteins of the ECM. It confers elasticity to tissues, hence enabling them to stretch and recover their original state. As other elastomers,[1, 2] elastin is predominantly characterized by long polymeric amorphous chains. In tissue, these chains are covalently cross-linked at intervals by desmosine and isodesmosine linkages, formed by the condensation of three allysine plus one lysine condensated amino acid side chains. This conformation allows the almost free mobility of the chains and thus ensures a considerable degree of stretching under mechanical stress, while still

guaranteeing recovery of the original conformation due to inter-chain covalent bonds.

The remarkable elastic properties of elastin depend critically on the presence of water: the dehydrated protein is stiff and brittle and the mechanisms of interaction with water were a target of the present investigations. In order to study the conformational properties of the protein and the role of water in determining its supramolecular structure, a water-soluble monomeric form, α-elastin, was prepared from porcine aorta by treatment with oxalic acid, which breaks covalent desmosine linkages.[3] This process restores approximately a quarter of lysine residues lost during fibrillogenesis from the soluble form of elastin secreted by the cell, tropoelastin. Although the behavior of elastin in aqueous solution is dominated by hydrophobic interactions, there is some electrostatic interaction and solutions are most stable at pH 7.3, where the polar amino acid residues such as lysine and tyrosine side chains are in their neutral form (pK_a 10.28 and 10.07, respectively). Aqueous elastin solutions exhibit coacervation at around body temperature,[4] and it has been postulated that this process could constitute an initial step in fibre formation in tissues,[5] although a number of glycoproteins also form a scaffold for fibre formation. *In vitro*, hydrophobic aggregates consisting of elastin molecules aligned along their hydrophobic domains (GVGVP peptide sequences) develop and precede the formation of mature fibres. Although numerous investigations have been carried out on the process of fibre formation, there is still notable lack of information about the molecular mechanisms determining the dynamics of supramolecular organization.

Infrared (IR) absorption spectroscopy is a valuable tool to investigate protein dynamics, because of its sensitivity to secondary structure, site-specific coordination, solvent accessibility and structural stability.[6-8] The protein backbone vibrations give rise to three fundamental IR bands: amide I (mainly peptide C=O stretching) at 1690-1620 cm^{-1}, amide II (C–N stretching coupled with N–H bending) at ca. 1550 cm^{-1} and amide III (C–N stretching, N–H bending and C–C stretching) at ca. 1300 cm^{-1}, which are the most informative bands for elucidating protein conformation. In the vibrational spectrum of proteins, the amide I band is inhomogeneously broadened, owing to the presence of different classes of peptide C=O oscillators that probe different protein conformations and molecular environments. This makes IR spectroscopy a powerful tool for studying local sites and their dynamics in complex systems. Nonlinear methods provide more information than linear experiments, e.g. using Fourier transform infrared (FTIR) spectroscopy. They can reveal coupling between vibrational modes and give access to the temporal evolution of vibrational frequencies and anisotropies with sub-picosecond time resolution, hence enabling direct measurement of fast structural/environmental fluctuations.

In this study, we applied time-resolved IR spectroscopy to study the coacervation of α-elastin in buffer solution. Light scattering measurements were performed initially to investigate the reversibility of the coacervation process and, on the basis of these results, light microscopy was used to investigate the formation of an unstable coacervate at temperatures above 46°C and of a stable

coacervate above 85°C. FTIR spectroscopy was employed to probe the amide I protein backbone vibration of α-elastin during both stages of coacervation and nonlinear pump-probe IR spectroscopy was used to determine the associated molecular structure and dynamics.

2. Materials and Methods

2.1 Materials. α-Elastin was prepared according to a procedure refined in our laboratory (see Supporting Information). Dried α-elastin was dissolved in a solution of PBS (composition in g/l: NaCl, 8.0; KCl, 0.2; Na_2HPO_4, 1.15; KH_2PO_4, 0.2; pH 7.3) in D_2O at a concentration ranging between 17 and 50 mg/ml. The use of D_2O enables interference from the water bending absorption[9] in the amide I (A-I) spectral region to be avoided, while preventing the formation of other protein structures different from those expected *in vivo*.

2.2 Microscopy and Spectroscopy. A lab-built aluminium cell for temperature-controlled spectroscopy was used in all measurements. It consisted of two calcium fluoride windows separated by a Teflon spacer, giving a path length of 50 μm. The cell body was electrically heated above room temperature using two electrical resistors on opposite sides of the cell. A thermocouple was used to measure the temperature in proximity to the sample with a precision of ±0.2 °C.

The formation of a α-elastin coacervate was visualized in light microscope images, obtained using an Olympus BH2 optical microscope, with a 10× Olympus MPlan objective coupled to an Optikam B5 5Mpxl digital camera.

UV-visible absorption spectra were collected using a PerkinElmer Lambda 950 spectrophotometer, with a 2 nm resolution in the range 250–600 nm. Coacervation was assayed by monitoring turbidity through light scattering at 400 nm, away from any absorption signal of the sample. Light scattering was assayed at selected temperatures between approximately 25 and 85°C, after a 20 minute-thermalization period at each temperature.

Fourier transform infrared (FTIR) absorption spectra were collected in transmission mode using a Bruker Alpha-T FTIR spectrometer and the cell described above. OPUS v. 6.5 software was used for acquisition and manipulation of the data. Each IR spectrum was obtained by co-adding 32 scans measured over the range 800–4000 cm^{-1} at 2 cm^{-1} resolution.

Ultrafast nonlinear IR spectroscopy measurements were performed using the apparatus described in previous works.[10, 11] Essentially, it is based on a Ti:sapphire regenerative amplifier (Legend Elite Coherent), providing 40 fs pulses centred at 810 nm, with a 3.5 mJ energy per pulse and 1 KHz repetition rate. A portion of the output of the amplifier is used to pump two independent optical parametric amplifiers (OPA) - a commercial system (TOPAS-800, Light-Conversion) which produces the pump pulses, with a 6 μm central wavelength and 4 μJ energy/pulse, and a white light-seeded lab-built OPA which generates probe and reference pulses. The pump pulse is used to excite specific molecular vibrations, while the probe pulse follows their relaxation. Spectra at different pump-probe delays were collected by sending the pump pulse trough a computer controlled motorized stage before being overlapped to the probe at

the sample position. The reference beam was directed through the sample at a slightly shifted position (along the vertical axis) relative to the pump and probe beams, which were focused on a spot of ca. 100μm. After passing through the sample, both probe and reference pulses were spectrally dispersed by a spectrometer (TRIAX 180, HORIBA JobinYvon) and sent separately to a double 32-channel mercury cadmium telluride (MCT) detector (InfraRedAssociates Inc.). The ratio of the probe-to-reference spectrum gives the differential absorption spectrum, ΔA, which is recorded as a function of the pump-probe time delay. Before the delay stage, the polarization of the pump beam was selected using a half-wave plate and set, for each delay time, parallel and then perpendicular to the probe. For each sample, pump-probe polarized spectra were collected and the vibrational relaxation and spectral anisotropy responses were derived.

The nonlinear response of the protein A-I vibration was obtained using broadband pump and probe pulses. In order to disentangle the contribution of the different components underlying the broad A-I absorption, narrowband excitation was used. Pump pulses with a spectral bandwidth (full width at half maximum, FWHM) of 17 cm^{-1} were obtained using a Fabry–Pérot filter,[12] which also reduced the energy to 200 nJ/pulse. A 150 l/mm grating provided a spectral resolution of approximately 4 cm^{-1}. Each nonlinear spectrum was frequency-calibrated based on the corresponding FTIR spectrum. Nonlinear IR measurements of α-elastin solutions were performed at two temperatures, 25°C - before coacervation, and 46°C - after coacervation, as previously reported for tropoelastin.

2.3 Data Analysis. The measured decay of induced absorption ΔA over delay time between pump and probe pulses is due to the relaxation of the vibrational state population and the reorientation of the vibrational transition dipole moment. This latter motion follows the orientational dynamics of the system and causes a decay of spectral anisotropy.[12-14]

Experimentally, it is possible to separately investigate the vibrational and rotational dynamics by performing pump-probe polarization-resolved measurements using both parallel $\Delta A_{\parallel}$ and perpendicular $\Delta A_{\perp}$ configurations. The population decay and spectral anisotropy decay are calculated using the following expressions

$$\Delta A_{MAS}(t) = \frac{\Delta A_{\parallel}(\mathrm{t}) + 2\Delta A_{\perp}(\mathrm{t})}{3} \quad (1)$$

and

$$R(t) = \frac{\Delta A_{\parallel}(\mathrm{t}) - \Delta A_{\perp}(\mathrm{t})}{\Delta A_{\parallel}(\mathrm{t}) + 2\Delta A_{\perp}(\mathrm{t})}, \quad (2)$$

where $\Delta A_{MAS}(t)$ indicates the differential signal at the magic angle (MAS = 54.7°) and $R(t)$ is the anisotropy. Pump-probe polarization-resolved measurements were performed using both broadband and narrowband excitation. The latter experimental configuration enables the characteristic vibrational lifetime and rotational dynamics for each A-I band component to be singled out. As a side effect, a narrower excitation pulse causes a loss in temporal resolution (down to 800 fs), because the pump pulse undergoes a time broadening when passing

through the Fabry–Pérot filter. As a consequence, the fit analysis had a starting point at approximately 800 fs.
The evolution of induced absorption on the picosecond time scale is due to the vibrational dynamics associated with the relevant (A-I) mode and can be fit through a single exponential decay. Parameters of the fit function

$$\Delta A(t) = A \exp[-(t/\tau)] \quad (3)$$

are the amplitude factor A and the vibrational lifetime constant τ.
We used the same function to analyze the decay of spectral anisotropy. Note that at the time zero, the molecular α-elastin solution should be a truly isotropic system with $\Delta A_{\perp} = \left(\frac{1}{3}\right)\Delta A_{\parallel}$ and $A_{t=0} = 0.4$; however, for the coacervate this may not be valid. As for the analysis of vibrational dynamics, the ultrafast response (<800 fs) was discarded and the longer picosecond response was fit to a single exponential function (eq. 3) to derive the relevant time scales.

3. Results

3.1 Light Scattering. Figure 1 shows the evolution of the UV-visible absorption spectrum of a α-elastin solution as a function of temperature in the range 25–53 °C. The spectrum has a prominent band at 200 nm (not shown) due to the absorption of the peptide bond and a band at 276 nm due to the aromatic amino acid tyrosine,[15] making up ~0.2% of the elastin amino acid composition. An increase in the background at longer wavelengths is observed at increasing temperature, owing to an increase in light scattering of the solution as the coacervate forms.[4]

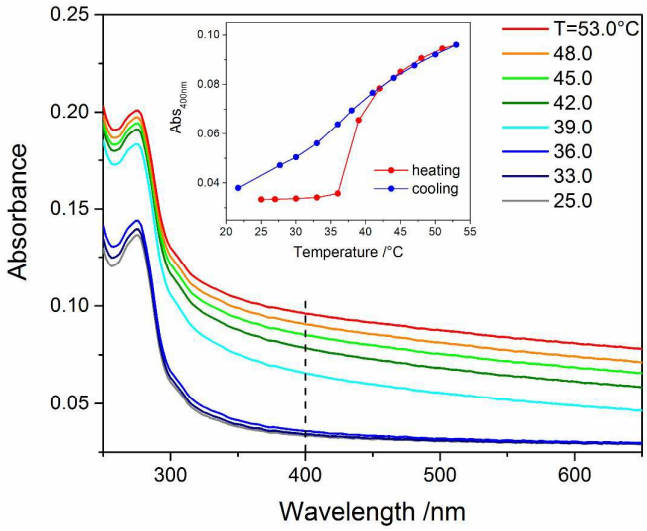

Figure 1. Evolution of the UV-visible absorption spectrum of α-elastin in PBS-D_2O as a function of temperature, in the range 25.0 to 53.0°C. Each spectrum was measured after a 20 minute-thermalization period at each temperature. Band at 276 nm: tyrosine. Turbidity was assayed through light scattering at 400 nm (dashed line). Inset: plot of the absorbance at 400 nm versus temperature for both heating (red symbols) and cooling series (blue symbols).

A plot of the UV-visible absorption at 400 nm versus temperature for both heating and cooling series (see Figure 1 inset) shows the reversibility of the coacervation process by a hysteresis cycle with inflection points at 39 and 37°C, respectively. These values are close to the coacervation temperature previously found for tropoelastin.[4] Note that a similar evolution is observed for the UV-visible absorbance at different wavelengths, in the range 370 to 650 nm, as a function of temperature (Figure SI-1 in Supporting Information).

If the sample was not thermalized at each temperature and higher temperatures (up to ca. 80°C) were reached for the solution, a double sigmoidal curve was instead obtained with inflection points at 42.2 and 62.3°C (Figure SI-2). This indicates that a rapid heating of the solution, at a rate of 0.96°C/min, shifts the coacervation temperature upwards (by ~3°C), as the sample has not stabilized at each temperature, and that a second process occurs at higher temperature (>60°C). Cooling the system down to room temperature immediately did not restore the background observed at the beginning of the experiment for room temperature and no sigmoid was observed (Figure SI-2 inset), indicating the insolubility of the coacervate that forms above 60°C.
Figure 2 shows visible light images of a α-elastin solution at room temperature and after being thermalized at 46 and 85°C, i.e. above the first and the second inflection points, respectively.

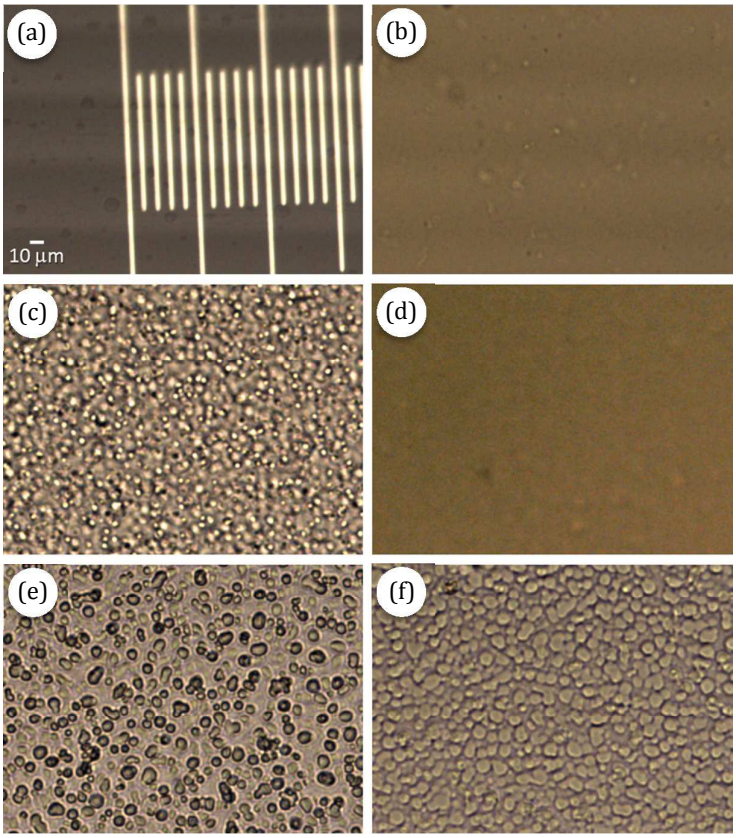

Figure 2. Visible light images of α-elastin in PBS-D_2O. (a) Calibration cover slip. (b) T = 25°C at the start of the experiment; clear, transparent solution. (c) 46°C after thermalization; globules of <5 µm diameter are visible. (d) 25°C after heating to 46°C; globules dissolve and the solution is clear. (e) 85°C after thermalization; bigger droplets of up to 10 µm diameter, some with peanut-

like shape are visible. (f) 25°C after heating up to 85°C; droplets persist as the aggregation proceeds and becomes irreversible.

Photomicrographs clearly show the onset of a liquid–liquid phase separation in the coacervation process. The freshly prepared solution is clear at room temperature (Figure 2b), then heating up to 46°C a myriad of drops of a few μm in diameter are apparent (Figure 2c). They rapidly dissolve upon cooling back to room temperature (Figure 2d). Upon heating again up to 85°C, globules of up to 10 μm diameter are observed, with some bigger droplets assuming "peanut-like" shapes (Figure 2e). Similar behavior has been observed in tropoelastin coacervates.[16] Cooling back to room temperature, the sample remains turbid and even after 2 days the droplets persist and increase in number (Figure 2f).
Light scattering of the α-elastin solution was assayed over time at selected temperatures (Figure SI-3) and a decay was observed for 37.5, 40 and 60°C, with a maximum of light scattering at 40°C (near coacervation), whilst no change was apparent at the lower and higher temperature ends of the range. This indicates that the process is dynamic and can be tuned to favour one (molecular solution) or the other (coacervate) state of the system. The data at 85°C show no changes in turbidity over time, hence indicating that a stable coacervate has formed.

3.2 FTIR Absorption. Figure 3a shows the evolution of the FTIR spectrum in the region of the amide I and II bands as a function of temperature, in the range 25–60 °C.

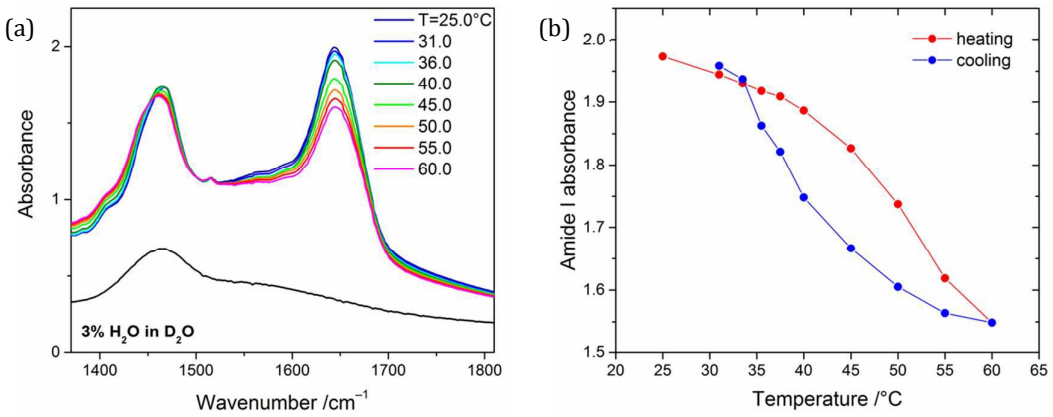

Figure 3. (a) Evolution of the FTIR spectrum of α-elastin in PBS-D_2O as a function of temperature, in the range 25–60 °C. Bands at 1465 and 1644 cm^{-1}: δ(CND) and amide I, respectively. Black line: spectrum of a 3% v/v H_2O/D_2O solution showing the band of HOD bending at ~1450 cm^{-1} and no contribution in the region of the amide I band. (b) Plot of the amide I peak intensity (height) as a function of temperature for both heating (red symbols) and cooling series (blue symbols).

The A-I band at 1644 cm^{-1} is primarily due to the C=O stretching of the amide group in the α-elastin backbone and is highly sensitive to structural and conformational changes as well as to molecular interactions of the protein. By increasing the temperature up to 60°C, no shift is observed but instead a notable decrease in intensity at 1644 cm^{-1} accompanied by a band broadening on both sides of the maximum.

No significant signal is observed near 1550 cm^{-1}, in the region of the amide II band, which is due to an out-of-phase mixture of C–N stretching and N–H in-plane bending of the protein backbone. Upon deuteration of the amide group in D_2O, the δ(ND) bending mode undergoes a red-shift to 1465 cm^{-1}.[17] In the same region, the absorption due to the δ(HOD) bending of HOD molecules that arise from H_2O–D_2O exchange is expected.[18] The spectrum of a 3% v/v H_2O/D_2O solution (Figure 3a) shows the δ(HOD) band at the same wavenumbers as the amide II band of α-elastin, hence ruling out the possibility of using the amide II to study coacervation.

Here we focused on the A-I band, which contains no contributions other than from α-elastin; this was confirmed by a measurement on a PBS-D_2O solution which showed no change in intensity of the 'solvent' spectrum in the region of the A-I band (Figure SI-4). In the absence of PBS, only a minor change in the A-I band is observed (Figure SI-5); this result confirms previous findings showing no coacervation of tropoelastin in the absence of NaCl[4] and indicates that the large decrease of intensity for the A-I band (Figure 3a) is only due to coacervation. A plot of the peak maximum versus temperature for both heating and cooling series (Figure 3b) shows hysteresis, confirming the light scattering results above (Figure 1 inset) and the fact that heating up the sample below 60°C and then cooling it down to room temperature produces a completely reversible coacervation.

3.3 Transient IR Absorption. To study the effect of coacervation on the A-I vibrational lifetimes and gain information about the protein conformational change, we measured transient IR spectra of α-elastin solutions at two temperatures, 25 (fresh clear solution) and 46°C (reversible aggregation of α-elastin forming small globules). Nonlinear IR measurements of the coacervate were performed at 46°C, just above the reversible coacervation point, since this ensured lower turbidity, hence lower scattering, and higher homogeneity of the sample within the illuminated spot of 100 μm size.
All measurements were executed in a D_2O equilibrated sample. The effect of D_2O on the thermodynamic properties of several elastin-type polypeptides has been studied by Luan and Urry using DSC.[19] They found that D_2O enhances the hydrophobicity, lowering the temperature of the inverse (temperature) transition by ~2°C and increasing the heat of transition by ~10%. The small magnitude of these effects indicates that there is no marked change in protein conformation.

Figure 4 shows the evolution of the IR transient spectrum of α-elastin at 25°C for different pump-probe delays. Each transient response has a positive low-frequency part due to the excited state absorption (ESA; transition $\nu_2 \leftarrow \nu_1$; Figure 4 inset) and a negative high-frequency part originating from the bleaching ($\nu_1 \leftarrow \nu_0$) and stimulated emission ($\nu_0 \leftarrow \nu_1$).

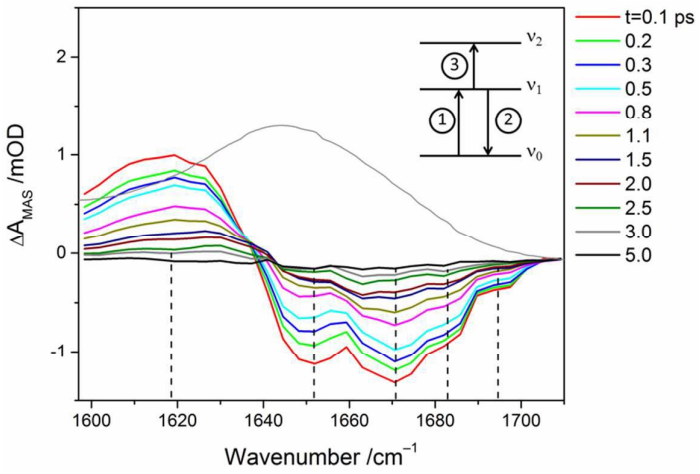

Figure 4. Evolution of the broadband nonlinear IR spectrum of α-elastin in PBS-D_2O as a function of pump-probe delay in the range 0.1–5 ps, at 25°C. Thin gray line: FTIR spectrum. Dashed lines indicate distinct absorption peaks identified by minima in the nonlinear spectrum. Inset: vibrational energy level diagram. Note the energy difference due to anharmonicity between bleaching (1) and stimulated emission (2) transitions vs excited state absorption (3).

Whilst the linear FTIR spectrum (gray line in Figure 4) contains fundamental state contributions from various A-I components at close frequencies, hence resulting in a featureless A-I profile, the negative part of the transient response shows at least four distinct components, at ~1650, 1670, 1680 and 1695 cm^{-1}. At longer pump-probe delays (>1.5 ps from excitation), a small 'dip' at ca. 1620 cm^{-1} becomes apparent, indicating a possible additional component. The observation of a structured broadband nonlinear IR spectrum in the amide I region is very significant because it reveals the presence of at least four distinct components, plausibly corresponding to an inhomogeneous static distribution of different protein structures. It is worth pointing out that the observed structured bleaching in the broadband A-I spectrum is not common to other large proteins such as Concanavalin A (Con A), RNaseA, Ubiquitin and Myoglobin.[13, 20] The frequency separation between minima above 1640 cm^{-1} suggests that the anharmonicity Δ, i.e. the difference in frequency between maximum and minimum of each A-I component, is in the range of 15–20 cm^{-1} (Figure SI-6; Table SI-1). Due to a spectral overlap between A-I sub-components, an accurate estimation of Δ for each contribution is not feasible here. The value of Δ for deuterated N-methylacetamide (NMA), which is a model for the amide bond, has previously been estimated to be 16 cm^{-1},[21] i.e. in the range found here for α-elastin.

Figure 4 clearly indicates a strong superposition and mixing of carbonyl stretching sub-bands. However, it also suggests that an excitation frequency-resolved approach is necessary to disentangle the four distinct components and their relative dynamics. We recorded a series of transient spectra by scanning the excitation frequency (with a 17 cm^{-1} FWHM) across the A-I absorption band (FWHM ~ 60 cm^{-1}).

Figure 5 shows the spectra obtained through directly exciting individual components of the A-I band at 1614, 1642, 1670 and 1680 cm^{-1} at 1 ps pump-probe delay. Two temperatures were compared, 25 and 46°C, i.e. below and above the coacervation temperature.

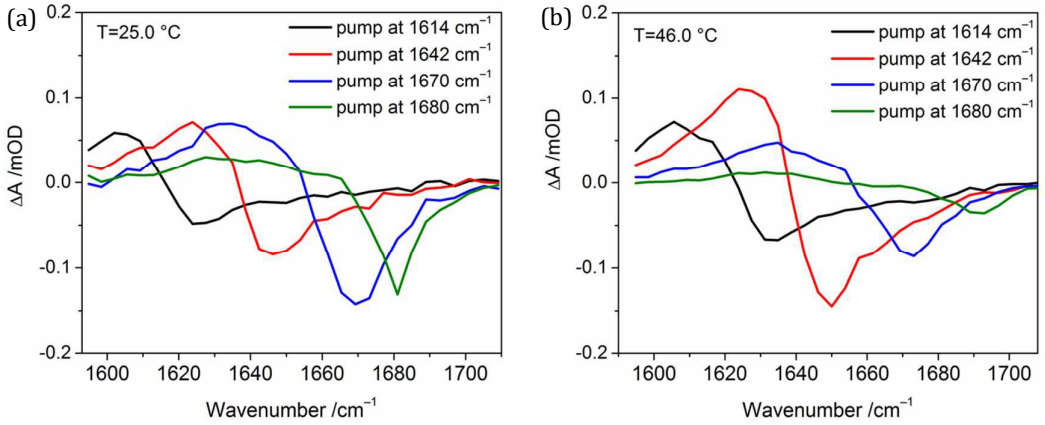

Figure 5. Transient spectra of α-elastin in PBS-D_2O measured at 1 ps from excitation, with the pump centred at selected wavenumbers (indicated in legend), at (a) 25°C and (b) 46°C.

Below the coacervation temperature (Figure 5a), the transient profile measured with the pump centred at 1680 cm^{-1} has a minimum at 1680 cm^{-1}, whilst above the coacervation temperature (Figure 5b) at the same excitation conditions, the minimum is at 1695 cm^{-1} and is less pronounced.
Similarly, the profile for 1670 cm^{-1} has a minimum at ~1670 cm^{-1} at 25°C but this slightly blue-shifts, broadens and decreases in intensity at 46°C. The profiles for 1642 and 1614 cm^{-1} also have a minimum that shifts upwards, however it becomes more pronounced towards higher temperature, particularly for the profile at 1642 cm^{-1}. All these spectral variations upon varying temperature indicate a change in protein structure upon formation of the coacervate. At each temperature, the overall appearance of the profiles is maintained at longer pump-probe delays, ruling out the presence of conformational changes within the short vibrational lifetime.

3.4 Ultrafast Dynamics. Figure 6 and 7 show the vibrational kinetics of a α-elastin solution measured at the minima of the narrowband transient spectra (Figure 5), at 25 and 46°C, respectively. The corresponding decay times derived from fitting to an exponential decay are listed in Table 1.

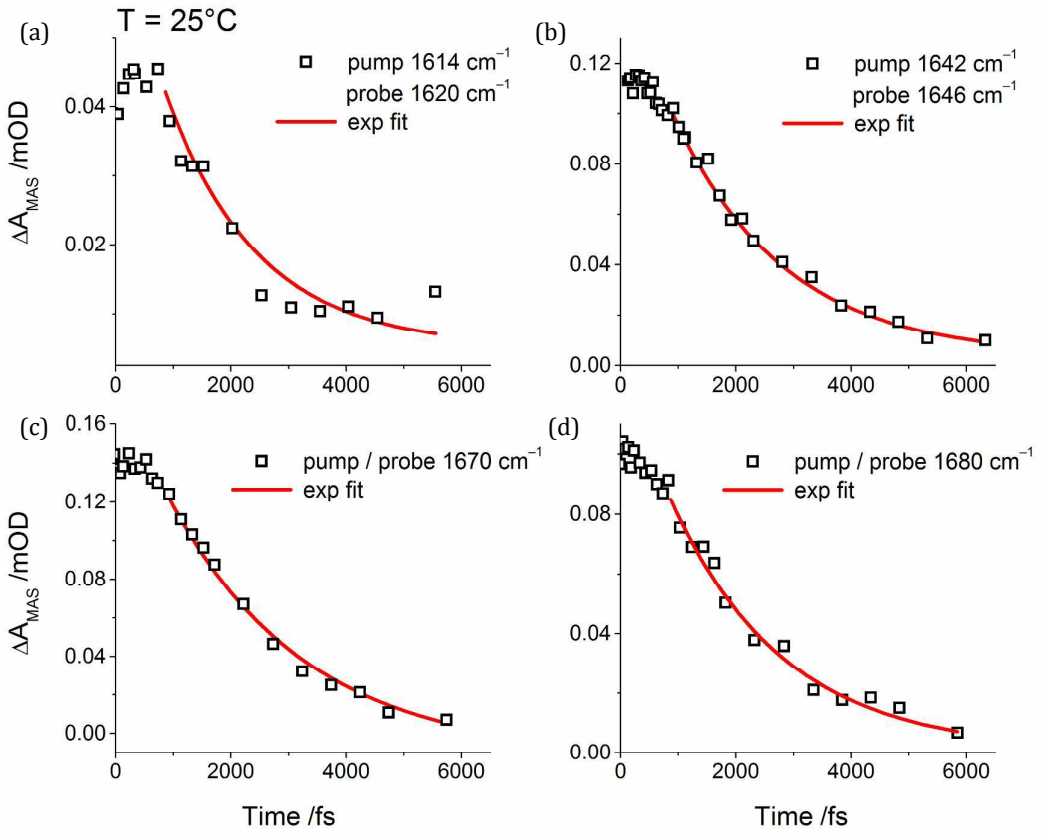

Figure 6. Vibrational kinetics of α-elastin in PBS-D_2O measured at 25°C. Each plot corresponds to bleaching dynamics with pump and probe frequencies set to (a) 1614/1620 cm^{-1}; (b) 1642/1646 cm^{-1}; (c) 1670/1670 cm^{-1}; (d) 1680/1680 cm^{-1}. Red lines: exponential decay fit results; the vibrational decay times are listed in Table 1.

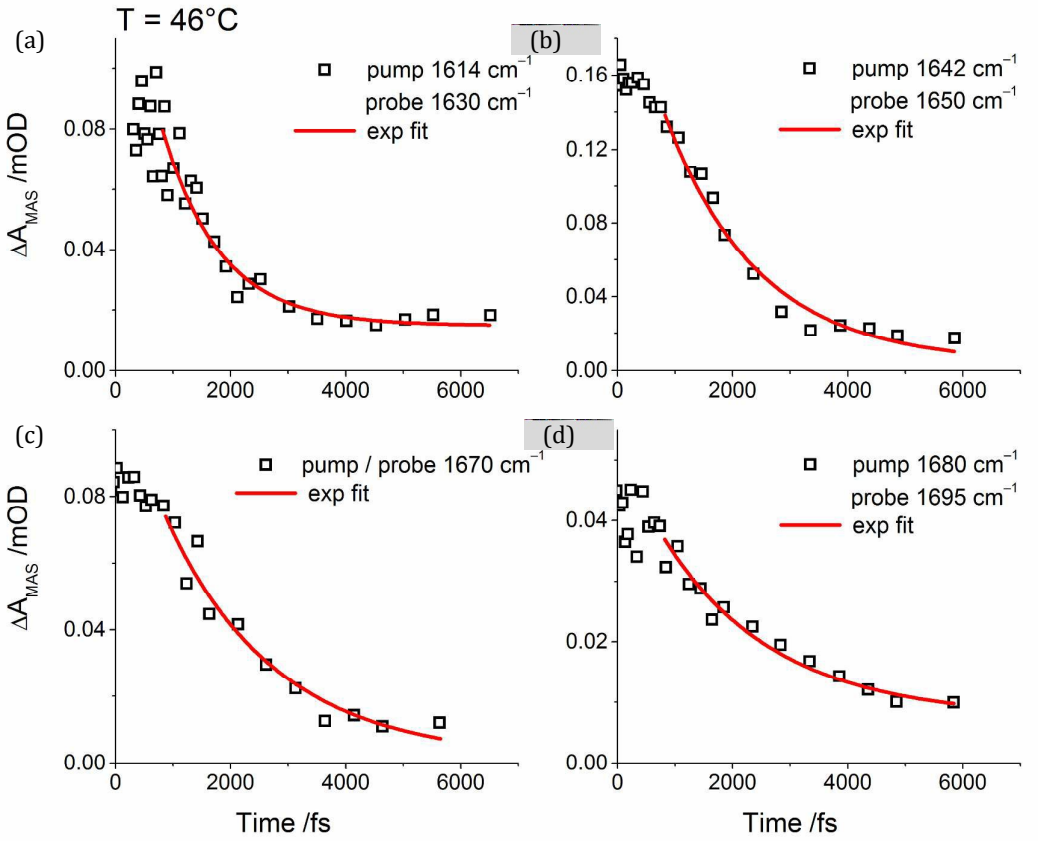

Figure 7. Vibrational kinetics of α-elastin in PBS-D_2O measured at 46°C. Each plot corresponds to bleaching dynamics with pump and probe frequencies set to (a) 1614/1630 cm^{-1}; (b) 1642/1650 cm^{-1}; (c) 1670/1670 cm^{-1}; (d) 1680/1695 cm^{-1}. Red lines: exponential decay fit results; the vibrational decay times are listed in Table 1.

As already apparent in Figure 5, the component excited at 1642 cm^{-1} has a two-fold increase in amplitude upon coacervation, whilst both higher frequency components decrease (and the lowest frequency band increases as the ESA positive part of the signal rises). Assuming a similar transition dipole moment for all A-I sub-bands, it is possible to correlate the increase (or decrease) in amplitude of the band to a parallel increase (or decrease) in the corresponding population of protein conformations. Hence, the two components on the low frequency side, which gain in intensity upon coacervation at the expenses of the two components at higher frequency, indicate a parallel increase in their vibrational population at the expense of the others.

Similarly to other proteins,[22] α-elastin solutions show decay of the amide I vibration in the picosecond domain (see Table 1). Although a unique and definitive model for all proteins has not yet been developed, the value of decay time depends on the carbonyl group environment and on the extent of the exciton coupling among neighbouring transition dipoles.[11, 21, 23] It can be seen (Table 1) that the decay is faster upon coacervation, with the exception of the component at 1680 cm^{-1} which remains essentially unchanged - although the probe frequency shifts to higher frequency. The fastest vibrational decay, with a time constant of 1.02 ps (at 46°C), is observed when the excitation frequency is

set to 1614 cm^{-1}, suggesting that the excited dipole is essentially isolated and decoupled from other carbonyl vibrations decaying on a longer time scale.

Besides the vibrational lifetime of the distinct A-I components, we also analyzed the anisotropy decays, which are particularly sensitive to dephasing processes and changes in orientation among dipole moments, in order to attribute the observed intramolecular modes to specific secondary structures of the protein. The anisotropy kinetics of α-elastin solutions at 25 and 46°C are shown in Figure 8 and SI-8, respectively. The corresponding decay times derived from fitting to an exponential decay are listed in Table 1.

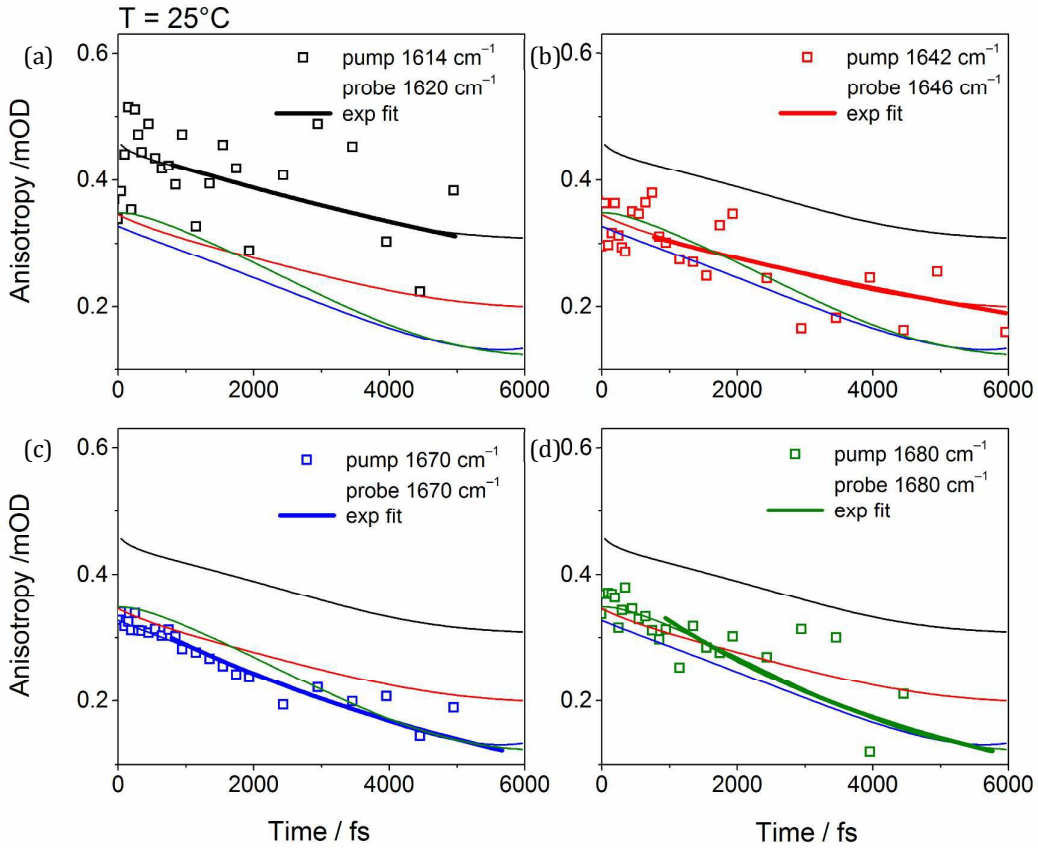

Figure 8. Anisotropy kinetics of α-elastin in PBS-D_2O measured at 25°C. Selected pump and probe frequencies were (a) 1614/1620 cm^{-1}; (b) 1642/1646 cm^{-1}; (c) 1670/1670 cm^{-1}; (d) 1680/1680 cm^{-1}. In each plot, empty symbols denote experimental data and matched color lines are the exponential decay fit results; other color lines represent the results of fit analysis for the other panels. The anisotropy decay times are listed in Table 1.

Table 1. Parameters[a] of the Exponential Fit Applied to the (a) Vibrational Kinetics and (b) Anisotropy Kinetics of α-Elastin Solutions at 25 and 46°C.

(a) Vibrational Kinetics					
T = 25°C			T = 46°C		
Pump/probe /cm^{-1}	A	τ_v /ps	Pump/probe /cm^{-1}	A	τ_v /ps
1614/1620	0.09	1.52	1614/1630	0.08	1.02
1642/1646	0.13	1.93	1642/1650	0.24	1.63
1670/1670	0.23	2.31	1670/1670	0.13	1.91
1680/1680	0.14	1.94	1680/1695	0.05	1.95
(b) Anisotropy Kinetics					
T = 25°C			T = 46°C		
Pump/probe /cm^{-1}	τ_{an} /ps		Pump/probe /cm^{-1}	τ_{an} /ps	
1614/1620	11.5		1614/1630	< 3	
1642/1646	11.3		1642/1650		
1670/1670	6.8		1670/1670		
1680/1680	4.7		1680/1695		

[a] Values are reported as A, pre-exponential coefficient; τ_v and τ_{an}, vibrational and anisotropy time constant, respectively. Errors are ±0.02 ps for the vibrational decay times and ±0.4 ps for the anisotropy decay times. For the anisotropy decays, A was fixed to the value of 0.4.

The dipole moment of large proteins such as α-elastin undergoes rotational diffusion on a μs–ms time scale; within the short vibrational lifetime of the A-I mode (5-6 ps), the presence of this slower motion cannot be detected. Besides slow rotational diffusion, fast picosecond or sub-picosecond anisotropy decay has already been observed for the A-I modes in highly ordered proteins.[21, 24] Here, the A-I modes of α-elastin (Figure 8 and Table 1) show anisotropy time constants of ~11 ps for the bands excited at 1614 and 1642 cm^{-1}, while the bands excited at 1670 and 1680 cm^{-1} have a slightly faster anisotropy decay, with ~5-7 ps time constant. There are two possible sources of spectral anisotropy decay on a picosecond time scale: i) local structural fluctuations/rearrangements of the peptide backbone, which cause changes in the orientation of the amide I transition dipoles; ii) resonant energy transfer among adjacent amide groups. Both effects are expected to become stronger as the temperature rises due to the higher number of populated quantum states that are close in energy (better for energy transfer) and Brownian fluctuation and motion of the environment. The data in Table 1 show that, at 46°C, the anisotropy decay is remarkably shorter (<3 ps) for all A-I components. Note that at 46°C, anisotropy decays are not detectable above 4 ps (Figure SI-8); although the small time range does not enable an accurate fit analysis of the decays, substantial differences are not observed among the four A-I components.

4. Discussion

Analysis of the transient spectra of α-elastin solutions at different temperatures, below and above the (reversible) coacervation temperature, enabled the identification of distinct contributions to the A-I band in the IR spectrum. Transient IR measurements with narrowband excitation revealed characteristic spectral changes in these components, which give molecular insights into the protein conformational changes associated with coacervation. We shall first discuss details of the evolution in A-I spectral components and their assignment to specific structural motifs, and then endeavour to provide an interpretation of the results in terms of conformational changes of α-elastin.

Band at 1614 cm^{-1}. The slower anisotropy decay determined for this component ($\tau_{an} \sim 11$ ps; Table 1) suggests an assignment to a closed-shell configuration that prevents fast H–D exchange dynamics with water hydrogens. Moreover, the fast vibrational decay (1.52 ps; Table 1) indicates that the corresponding dipole is essentially isolated and decoupled from other carbonyl vibrations and is not involved in any exciton, which is typical of large ordered structures.

This band has previously been assigned to an irregular β-turn in a Val-Pro-Gly sequence, which is a major repeat sequence in elastin.[25, 26] The authors studied the effect of changing the (side chain) size of the residue X in a GVG-XPG-VG sequence, with X being either Gly or Ala or Val. They found that for the elastin type with X = Val, the VPG sequence mainly forms a tight turn containing two intramolecular hydrogen bonds to the proline carbonyl, which red-shifts its spectral position. The anisotropy time constant that we found is consistent with a restricted motion due to the constraint exerted by intramolecular hydrogen bonds.

With increasing temperature, both vibrational and anisotropy dynamics (with τ_v of 1.02 ps and $\tau_{an} < 3$ ps) become faster, suggesting that tight turns made of three amino acids unfold and open to faster protein or water hydrogen exchange. The broadening of the corresponding transient signal (Figure 5) and the shift of the corresponding bleaching to higher frequencies at 46°C support the formation of β-turns made of four-to-five amino acids. In addition, a more opened structure of the entire protein to the water environment is favored with the coacervation.

Bands at 1640–1670 cm^{-1}. For the Val-Pro-Gly sequence, Lessing et al. assigned the bands at 1640 and 1670 cm^{-1} to the perpendicular and parallel modes of an anti-parallel β-sheet structure.[25] Generally, these modes are assigned to the in-phase C=O stretching of facing carbonyls across β-strands and to the in-phase C=O stretching of parallel nearest-neighbor carbonyls within the same strand, respectively.[13, 27] Narrowband transient measurements (Figure 5) show that the intensity of these bands is greater at 1670 cm^{-1} than at 1642 cm^{-1} at 25°C, but the ratio is reversed for the coacervate (at 46°C). This indicates opposite behaviors with changing temperature that can only arise from having two different conformers: if both modes pertained to the same β-sheet conformer, they would change in the same direction upon a change in temperature.

Based on α-elastin's amino acid composition (in aa %: Ala, 21%; Pro, 13%; Gly, 28%; Val, 12%; Lys, 4%; Leu, 7%; Tyr, 0.2%; Phe, 0.2%), different conformers may contribute to the band at 1640 cm^{-1}:

- β-turns of XPG sequences with X = glycine or alanine, which are lighter residues than valine, have been found to absorb up to 1635 cm^{-1};[25]
- tight proline-glycine turns with two-to-three residues per turn are highly sensitive to the hydrophobic character of the X residue in the PGX sequence,[28] hence further increasing the inhomogeneity of the β-turn signal. In the case of larger β-turns with up to five residues per turn, proline's transition dipole moments are less decoupled from closest-neighbor amide groups and participate to local modes that absorb at higher frequencies;
- in α-elastin, as in tropoelastin (α-elastin is essentially tropoelastin with telopeptides at either end missing and a few lysines involved in the formation of desmosine cross-links), inner alanine-lysine (AK) cross-linking domains have been isolated.[29, 30] These domains are identifiable in the protein primary structure by a starting short sequence of alanine residues, whose propensity to form stable α-helices and poly-proline structures (PPII) in water has been found to increase with increasing temperature. Alanine's α-helices in water absorb at 1640 and 1650 cm^{-1}, owing to parallel (A symmetry) and perpendicular modes (E1 degenerate) relative to the helix axis, respectively.[31] Left-handed PPII helices, also known to be the building blocks of the elastic triple-helix structure of collagen, absorb around 1630 cm^{-1}.[32]

Although the band at 1640 cm^{-1} seems to arise from multiple contributions, a different origin of the band at 1670 cm^{-1} has been suggested from circular dichroism (CD) measurements at different temperature. For several AK cross-linking domains and VPGVG hydrophobic domains,[28, 29, 33] an iso-elliptic point has been observed at ca. 207 nm, between the decreasing random coil absorption at 190 nm and the increasing signal at 210–220 nm due to more ordered α-helices and β-sheets structures. If the band at 1670 cm^{-1} can be assigned to random parts of the protein, the observed decrease in intensity of this band upon coacervation (Figure 5) would indicate that random coils unfold to form more ordered structures (in the coacervate) that absorb at lower frequencies.

Bands at 1680 and 1695 cm^{-1}. While internal carbonyl groups are mostly stabilized by intra-chain hydrogen bonds, external carbonyls are preferentially water-solvated. It has been shown that[34] the FTIR amide I band red-shifts upon formation of large excitonic peptide–peptide interactions (C=O···H–N) more than by hydrogen bonding to water molecules (C=O···H–O). Within this picture, the band at 1680 cm^{-1} can reliably be assigned to external solvated amides. This hypothesis is further confirmed by the fastest anisotropy decay found (τ_{an} = 4.7 ps): amides exposed to solvent show larger frequency fluctuations (inhomogeneity) which favor the coupling and energy transfer with nearby groups.[24] Also, the matching of the frequency difference between the 1680 and 1695 cm^{-1} components with the energy associated to the second H-bond to carbonyl group (≈15-20 cm^{-1}), along with the increase in intensity at 1695 cm^{-1} with increasing temperature (Figure 5), suggests an average loss of one H-bonded water molecule to external amides. This indicates that the solvent cage effect decreases at higher temperature, thus favoring extended unfolded

structures of α-elastin. In a cooperative frame, hydrophobic forces drive the alignment of protein strands and promote the formation of protein–protein H-bonds. The exclusion of water molecules between α-elastin molecules and the formation of H-bonds is a reversible process, as observed in the first stage of coacervation, and likely to give rise to different viscosity in the droplet and liquid phases. A further increase in temperature above 60°C likely leads to an irreversible process, where allysine residues are also involved in the formation of covalent linkages between neighboring elastin molecules.[1, 35]

Conclusions

Ultrafast nonlinear IR spectroscopy in the amide I region was used to study the coacervation of α-elastin in PBS-D_2O solution. Both broadband and narrowband approaches were employed in order to disentangle the information contained within the structured vibrational band shape. The broadband approach revealed the presence of at least four distinct contributions to the A-I band, whereas a selective excitation approach enabled to analyze them separately and to investigate the origin of the band broadening observed in the (linear) FTIR spectrum. Results showed that the coacervation of α-elastin leads to the formation of ordered structures, which absorb at lower frequency (ca. 1640 cm^{-1}) within the A-I band envelop, and to a reduced solvent cage effect, which was inferred by the increase in intensity of the higher frequencies component with increasing temperature.

The observed spectral changes, together with faster vibrational and anisotropy dynamics on a picosecond timescale at higher temperatures, suggest that the coacervation of α-elastin mediated by conformational dynamics of the protein is connected with the interplay of intra- and inter-molecular interactions whereby water has a major role.

Associated Content

The Supporting Information is available free of charge on the RSC Publications website at DOI: ...

Author Information

Contributions

F.P. and C.P.W. conceived, designed and supervised the project. E.G. purified and characterized the samples. E.R., A.L. and F.P. performed the experiments. E.R., M.D.D. and F.P. wrote the manuscript with input from all other authors.

Corresponding Authors

Correspondence to: Francesca Palombo (f.palombo@exeter.ac.uk)

Notes

The authors declare no competing financial interests.

Acknowledgements

The authors would like to thank Prof Maurizio Becucci at the Department of Chemistry, University of Firenze for his help in the acquisition of the light microscope images. The research leading to these results has received funding from LASERLAB-EUROPE (grant agreement no. 284464, EC's Seventh Framework Programme).

References

1. R. A. Anwar, *Biochem. Educ.*, 1990, **18**, 162-166.
2. S. M. Partridge, D. F. Elsden and J. Thomas, *Nature*, 1963, **197**, 1297-1298.
3. S. M. Partridge, H. F. Davis and G. S. Adair, *Biochem. J.*, 1955, **61**, 11-21.
4. B. Vrhovski, S. Jensen and A. S. Weiss, *Eur. J. Biochem. / FEBS*, 1997, **250**, 92-98.
5. A. J. Bailey, *J. Clin. Pathol.*, 1978, **31**, 10.
6. Z. Ganim, H. S. Chung, A. W. Smith, L. P. DeFlores, K. C. Jones and A. Tokmakoff, *Acc. Chem. Res.*, 2008, **41**, 432-441.
7. C. R. Baiz, M. Reppert and A. Tokmakoff, *J. Phys. Chem. A*, 2013, **117**, 5955-5961.
8. M. Cho, *Chem. Rev.*, 2008, **108**, 1331-1418.
9. http://www1.lsbu.ac.uk/water/water_vibrational_spectrum.html.
10. M. Lima, M. Candelaresi and P. Foggi, *J. Raman Spectrosc.*, 2013, **44**, 1470-1477.
11. M. Candelaresi, E. Ragnoni, C. Cappelli, A. Corozzi, M. Lima, S. Monti, B. Mennucci, F. Nuti, A. M. Papini and P. Foggi, *J. Phys. Chem. B*, 2013, **117**, 14226-14237.
12. P. Hamm and M. Zanni, *Concepts and Methods of 2D Infrared Spectroscopy*, Cambridge University Press, 2011.
13. M. D. Fayer, *Ultrafast Infrared Vibrational Spectroscopy*, CRC Press, 2013.
14. R. M. Hochstrasser, *Proc. Natl. Acad. Sci.*, 2007, **104**, 14190-14196.
15. https://www3.nd.edu/~aseriann/CHAP9B.html/sld013.htm.
16. A. W. Clarke, E. C. Arnspang, S. M. Mithieux, E. Korkmaz, F. Braet and A. S. Weiss, *Biochem.*, 2006, **45**, 9989-9996; L. D. Muiznieks, J. T. Cirulis, A. van der Horst, D. P. Reinhardt, G. J. L. Wuite, R. Pomès and F. W. Keeley, *Matrix Biol.*, 2014, **36**, 39-50.
17. M. Beer, H. B. Kessler and G. B. B. M. Sutherland, *J. Chem. Phys.*, 1958, **29**, 1097-1104.
18. S. Y. Venyaminov and F. G. Prendergast, *Anal. Biochem.*, 1997, **248**, 234-245.
19. C. H. Luan and D. W. Urry, *J. Phys. Chem.*, 1991, **95**, 7896-7900.
20. C. R. Baiz, M. Reppert and A. Tokmakoff, Introduction to Protein 2D IR Spectroscopy, web.mit.edu/~tokmakofflab/documents/Intro2DIR.pdf.
21. P. Hamm, M. Lim and R. M. Hochstrasser, *J. Phys. Chem. B*, 1998, **102**, 6123-6138.
22. A. Barth and C. Zscherp, *Q. Rev. Biophys.*, 2002, **35**, 369-430.
23. J.-H. Choi, S. Ham and M. Cho, *J. Chem. Phys.*, 2002, **117**, 6821-6832.
24. H. Torii, *Chem. Phys. Lett.*, 2000, **323**, 382-388.
25. J. Lessing, S. Roy, M. Reppert, M. Baer, D. Marx, T. L. C. Jansen, J. Knoester and A. Tokmakoff, *J. Am. Chem. Soc.*, 2012, **134**, 5032-5035.

26. J. Hilario, J. Kubelka and T. A. Keiderling, *J. Am. Chem. Soc.*, 2003, **125**, 7562-7574.
27. Y. Abe and S. Krimm, *Biopolymers*, 1972, **11**, 1817-1839.
28. Y. Cho, L. B. Sagle, S. Iimura, Y. Zhang, J. Kherb, A. Chilkoti, J. M. Scholtz and P. S. Cremer, *J. Am. Chem. Soc.*, 2009, **131**, 15188-15193.
29. A. M. Tamburro, A. Pepe and B. Bochicchio, *Biochemistry*, 2006, **45**, 9518-9530.
30. L. D. Muiznieks, S. E. Reichheld, E. E. Sitarz, M. Miao and F. W. Keeley, *Biopolymers*, 2015, **103**, 563-573.
31. S. Woutersen and P. Hamm, *J. Chem. Phys.*, 2001, **115**, 7737-7743.
32. A. A. Adzhubei, M. J. E. Sternberg and A. A. Makarov, *J. Mol. Biol.*, 2013, **425**, 2100-2132.
33. C. Nicolini, R. Ravindra, B. Ludolph and R. Winter, *Biophys. J.*, 2004, **86**, 1385-1392.
34. W. A. Herrebout, K. Clou and H. O. Desseyn, *J. Phys. Chem. A*, 2001, **105**, 4865-4881.
35. N. R. Davis and R. A. Anwar, *J. Chem. Phys.*, 1970, **92**, 3778-3782.